Virtual Mirrors: Non-Line-of-Sight Imaging Beyond the Third Bounce

Diego Royo[1], Talha Sultan[2], Adolfo Muñoz[1], Khadijeh Masumnia-Bisheh[2], Eric Brandt[2], Diego Gutierrez[1], Andreas Velten[2], Julio Marco[1]

[1] Afiliación: Graphics and Imaging Lab (GILab)
Instituto de Investigación en Ingeniería de Aragón (I3A)
Universidad de Zaragoza, Mariano Esquillor s/n, 50018, Zaragoza, Spain.
Tel. +34-976762707, e-mail: *droyo@unizar.es*
[2]Afiliación: Computational Optics Group
University of Wisconsin–Madison, Madison, WI, United States

Abstract

Non-line-of-sight (NLOS) imaging methods reconstruct scenes hidden around one corner using indirect third-bounce illumination on a visible relay surface. We show how diffuse hidden objects may exhibit specular behaviour in NLOS methods, and how fourth- and fifth-bounce illumination can encode useful information, such as imaging objects hidden around two corners.

Introduction

Non-line-of-sight (NLOS) imaging methods are able to reconstruct scenes hidden around a corner, with many applications in autonomous driving, remote sensing, or medical imaging. NLOS methods have presented promising advances with ultra-fast imaging devices, capturing light in motion with up to picosecond resolution [1] (Fig. 1a and Fig. 1b). Under this regime, time-gated NLOS imaging methods generate detailed reconstructions of hidden scenes by triangulating geometric positions using the time of flight of round-trip third-bounce illumination paths between a visible relay surface and scene [2].

Time-gated methods operate under the assumption of third-bounce-only illumination, with higher-order illumination degrading their reconstructions due to ambiguities in the time of flight of captured light, thus higher-order illumination is typically discarded. The phasor-field formulation [3], which we use throughout our work, uses third-bounce illumination in two steps. First, it computes the response of the scene to an arbitrary illumination function, based on the captured impulse response (Fig. 1c). Second, it computes an image of the hidden scene from the previous response at the relay surface, based on an imaging paradigm that interprets the time-resolved illumination captured at the relay surface as light arriving at the virtual aperture of a computational camera. This effectively converts the relay surface into a virtual line-of-sight (LOS) imaging system (Fig. 1d). Here it is key to understand that there are two domains, real and computational, where surfaces may exhibit different reflectance properties.

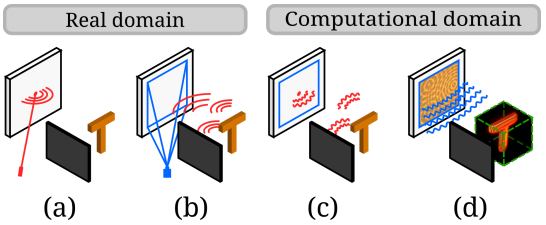

Fig. 1. (a) A laser device (red) emits a pulse towards a single point on the relay surface. (b) The resulting indirect illumination (i.e., the impulse response) is captured by an ultra-fast camera (blue). (c) Methods in the phasor-field framework operate on the impulse response to computationally illuminate the scene and (d) capture images of hidden objects from the relay surface.

In this work, we demonstrate how such higher-order bounces can be used to expand the capabilities of existing NLOS imaging systems, and overcome some of their current limitations. In particular, we draw a parallelism between Huygens' principle and the recent wave-based phasor-field NLOS imaging formulation. We intuitively show how, due to well-known wave interference principles, surfaces that are diffuse under visible light can behave like mirrors during the computational NLOS wave-based imaging process; we call such surfaces virtual mirrors. We implement existing computational camera models used in the phasor-field formulation (transient camera and confocal camera models [3]), and use virtual mirrors to extend their capabilities beyond the third bounce with novel applications, such as addressing the missing-cone problem in NLOS imaging [4] or looking around two corners.

Diffuse surfaces as virtual mirrors

A key observation in our work is that diffuse surfaces may exhibit specular properties in the computational NLOS wave imaging domain. In wave-based methods, time-resolved light transport $\mathcal{P}(\mathbf{x}, t)$ at any point $\mathbf{x}$ in the scene (t represents time) becomes a complex-valued phasor $\widehat{\mathcal{P}}(\mathbf{x}, \Omega) = \mathcal{F}\{\mathcal{P}(\mathbf{x}, t)\}$, which represents the amplitude and phase of the light wave, for frequencies Ω by applying a Fourier transform. When light travels from point $\mathbf{x}_a$ to point

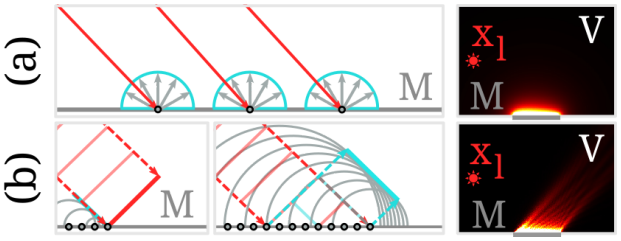

Fig. 2. (a) In the real domain, M scatters light from $\mathbf{x}_l$ diffusely. (b) In the computational domain, the processed signal corresponds to the specular reflection of $\mathbf{x}_l$ on M.

$\mathbf{x}_b$, the phasor $\widehat{\mathcal{P}}(\mathbf{x}_a, \Omega)$ undergoes a phase shift and attenuation modelled by the Rayleigh-Sommerfeld Diffraction (RSD) operator

$$\widehat{\mathcal{P}}(\mathbf{x}_b, \Omega) = \widehat{\mathcal{P}}(\mathbf{x}_a, \Omega) \frac{e^{ik|\mathbf{x}_b - \mathbf{x}_a|}}{|\mathbf{x}_b - \mathbf{x}_a|} \qquad (1)$$

where $|\mathbf{x}_b - \mathbf{x}_a|$ is the optical distance between $\mathbf{x}_a$ and $\mathbf{x}_b$, and the wavenumber $k = 2\pi\Omega/c$ (where c is the speed of light) is the conversion factor from optical distance to phase. The phase shift (numerator) and attenuation (denominator) form the RSD operator. Using this base, consider a point light at $\mathbf{x}_l$ whose emission is defined by the phasor $\widehat{\mathcal{P}}(\mathbf{x}_l, \Omega)$, and illuminates points $\mathbf{x}_m$ on a planar diffuse surface M, resulting in the phasors $\widehat{\mathcal{P}}(\mathbf{x}_m, \Omega)$. We can then compute the resulting phasor at any point $\mathbf{x}_v$ in a volume $\mathcal{V}$ as a superposition of phasors reflected from $\mathbf{x}_m$ using Eq. 1 from $\mathbf{x}_l$ to all points $\mathbf{x}_m \in M$, and then from each $\mathbf{x}_m$ to all $\mathbf{x}_v \in \mathcal{V}$. For a surface that is planar with respect the illumination wavelength Ω^{-1}, the phasors $\widehat{\mathcal{P}}(\mathbf{x}_v, \Omega)$ follow the specular reflection of $\widehat{\mathcal{P}}(\mathbf{x}_l, \Omega)$ on M as per Huygens' principle.

During the NLOS capture process (Fig. 2a, which corresponds to light transport Fig. 1a and 1b), the surface $\mathbf{x}_m$ scatters light from $\mathbf{x}_l$ in all directions. In the computational domain (Fig. 2b, using Eq. 1 in the process shown in Fig. 1c and 1d), the computed light transport now follows the specular direction.

We leverage virtual mirrors to address the missing-cone problem, a long-standing issue in NLOS imaging where certain surfaces in the scene have limited visibility [4]. We explain the missing-cone behaviour using virtual mirrors, and show a procedure to directly image hidden surfaces that have limited visibility when imaged using third-bounce methods. We refer the reader to our full paper for a detailed explanation of this procedure. We also use virtual mirrors to compute images of objects hidden around a *second* corner.

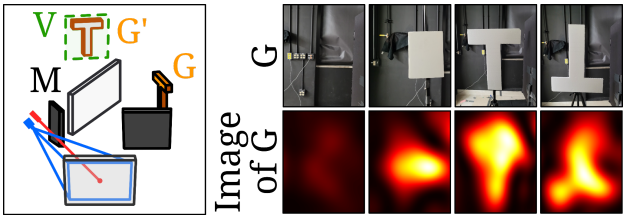

Fig. 3. Left: Setup to image G using a laser (red) and ultra-fast camera (blue) pointed towards the relay surface. G is hidden around two corners; we image the region V where G' (mirror image of G) is formed by M. Right: Setups (per column) and computed images of G.

Looking around two corners

We also leverage our virtual mirror reflections in the wave domain to image objects around a second corner using fifth-bounce illumination. Our key observation comes from the fact that diffuse planar surfaces may exhibit specular behaviour only in the computational domain. Thus, a planar surface creates a mirror image of objects in the hidden scene, *behind* such surface (like a real mirror). We image the region where this mirror image is formed, using the confocal camera model [3]. This is similar to third-bounce methods; but now uses fifth-bounce illumination by shifting the imaged region.

We design an experiment with a geometry G hidden around two corners from an ultra-fast laser and camera, both which are pointed towards the relay surface. A diffuse surface M is positioned and oriented such that the specular reflection of points in the relay surface on M reaches G, and vice-versa. We image the region V (Fig. 3), which shows the mirror image G' of G seen from the relay surface.

ACKNOWLEDGEMENTS

This work has received funding from the European Union's European Defense Fund Program (ENLIGHTEN project, No. 101103242), Gobierno de Aragón's Departamento de Ciencia, Universidad y Sociedad del Conocimiento (BLINDSIGHT project, ref. LMP30_21), MCIN/AEI/10.13039/501100011033 (Project PID2019-105004GB-I00), Air Force Office for Scientific Research (FA9550-21-1-0341), and by the National Science Foundation (1846884). Diego Royo was supported by a Gobierno de Aragón predoctoral grant.

REFERENCES

[1] VELTEN, A. et al., 2013. Femto-photography: capturing and visualizing the propagation of light. *ACM Transactions on Graphics*. 32(4), 1-8.

[2] VELTEN, A. et al., 2012. Recovering three-dimensional shape around a corner using ultrafast time-of-flight imaging. *Nature communications*. 3(1), 745.

[3] LIU, X. et al., 2019. Non-line-of-sight imaging using phasor-field virtual wave optics. *Nature*. 572(7771), 620-623.

[4] LIU, X. et al., 2019. Analysis of feature visibility in non-line-of-sight measurements. Proc. of the *IEEE/CVF Conference on Computer Vision and Pattern Recognition.*